Int. J. Electrochem. Sci., 14 **(2019)** 10016 – 10031, doi: 10.20964/2019.11.17

International Journal of
ELECTROCHEMICAL
SCIENCE
www.electrochemsci.org

Electrochemical Behavior of a Cactus Mucilage-Based Corrosion-Resistant Coating

L. D. López-León[1], *M. A. Juárez-Islas*[1], *A. Bassam*[2], *A. D. Pérez-Callejas*[3], *I. E. Castaneda-Robles*[1 *]

[1] Cuerpo Académico de Ingeniería Civil Sustentable y Tecnología de Materiales, Universidad Autónoma del Estado de Hidalgo, Mineral de la Reforma, México.
[2] Facultad de Ingeniera, Universidad Autónoma de Yucatán, Mérida, México
[3] Universidad Politécnica Francisco I. Madero, Francisco I Madero, México.
[*]E-mail: ivan_castaneda@uaeh.edu.mx

Received: 1 July 2019 / *Accepted:* 16 August 2019 / *Published:* 7 October 2019

This work presents an electrochemical evaluation of a proposed mucilage-based corrosion-resistant hybrid coating. The process started with the extraction of mucilage from *Opuntia streptacantha* and the formulation of 4 coatings containing 0.2, 0.3, 0.4 and 0.5 g of mucilage. The process continued with the coating of rebars through immersion. The rebars were allowed to dry, and then the coating thickness was measured by ultrasound. Optical micrographs were used to characterize the hybrid coating conditions after their evaluation. Working specimens were evaluated using electrochemical impedance spectroscopy and potentiodynamic polarization curves after 24 hours of immersion in a 3.5 wt.% NaCl solution. The mucilage-based hybrid coating reveals enhanced corrosion protection compared to steel without a coating. The obtained results show that the hybrid coating has favorable properties as a barrier due to its ability to obstruct the diffusion of aggressive species by trapping them in the coating structure, which avoids their adsorption on the metallic surface. This effect is due to the homogeneity of the mucilage in the coating, which acts as a corrosion inhibitor due to its semipermeable behavior, where only water molecules flow through its pores, showing promising results as a corrosion-resistant coating.

Keywords: Coating, Corrosion, Potentiodynamic polarization curves, Electrochemical impedance.

1. INTRODUCTION

The corrosion of reinforcement steel embedded in concrete has long been a concern [1-3]. The devastating impact of corrosion on the degradation of structural capacity degradation and reduction in the useful life of infrastructure shows that the human ability to mitigate steel corrosion is limited. Most of the corrosion mitigation methods are passive; ergo, they do not produce functional changes, such as a decrease in chloride ion concentration or changes in the concrete chemical composition. There is a

critical need to develop new corrosion mitigation strategies that are functionally effective for reinforced concrete structures.

Chloride-induced corrosion is one of the common causes of reinforced concrete structure degradation. It is a multi-stage process that starts with an ion influx through the concrete cover, chloride accumulation on the steel surface, and a disruption of the steel passivity, followed by corrosion initiation and propagation [3-4]. Any new mitigation alternative should be effective in one or several of these process stages. For instance, methods for chemical trapping of chloride ions would avoid their accumulation on the steel surface, slowing the passive layer degradation and reducing the steel corrosion rate. Similarly, there are methods for slowing corrosion initiation that also reduce the corrosion rates, such as designed electrochemical corrosion inhibitors, and could be implemented to allow functional changes throughout the steel-concrete interface [5,6]. Another alternative is to modify the steel composition.

The most effective method to protect a metal from corrosive agents is coating. However, it is significant to develop environmentally harmless coatings. Epoxy coating has been applied to protect steel reinforcement in concrete structures [7, 8]. However, its application is rather limited due to its susceptibility to damage by surface abrasion and wear [9]. The various methods to improve the corrosion resistance described in the literature are very diverse – from epoxy-coated rebars [10,11] to the use of galvanized steel [12-14] or stainless steel [15,16]. Nevertheless, they all have their drawbacks. Traditionally, chromate conversion coatings have been used for steel protection against corrosion, and such coatings also improve the adherence of further paint coatings. However, chromate conversion coatings are based on hexavalent chrome, which are toxic and are subject to restrictions [17]. Due to these toxicity issues, replacement using natural organic compounds such as seeds [18], plants and leaf extracts [19], nontoxic synthetic compounds (colorants) [20], rare earth elements [21], and organic compounds [22], which are cost effective, harmless, innocuous, easily obtainable and environmentally friendly, is required. Consequently, it is necessary to research alternative methods to improve steel corrosion resistance.

Nopal (*Opuntia ficus indica*) is a plant that grows in vast arid and semiarid areas. Currently, nopal is grown for commercial purposes in Mexico, Chile, Argentina, Morocco, Italy, and the states of California, Texas and Florida [23]. Nopal is a cactus of great agronomical importance in Mexico; there are 3 million hectares of native nopal and approximately 233,000 hectares of cultivated nopal; of these, 150,000 hectares are destined for human consumption, with a 139,193 ton annual production [24]. Different nopal species have been studied to determine the chemical compounds present in the plant to understand its properties and applications. Lee et al. (2002) assessed and related the antioxidant activity mechanisms of *Opuntia ficus-indica* var. Saboten, finding a high concentration of phenolic compounds (180.3 mg/g). Camarena-Rangel et al. (2017), found flavonoids and phenolic compounds through a phytochemical study of *Opuntia ficus-indica*, *Opuntia megacantha* and *Opuntia streptacantha callus*. Galati et al. (2005) studied *Opuntia ficus-indica* juice, finding ascorbic acid, polyphenols and flavonoids among its components, which presented antioxidant activity due to the phenolic compounds that were effective free radical eliminators. Nopal mucilage acted as a corrosion inhibitor for aluminum and steel in acidic solutions [25, 26]. Suarez and González et al. (2014) evaluated *Opuntia ficus* extract as a corrosion inhibitor for carbon steel in acidic media, reaching efficiencies as high as 94%. Torres-Acosta

et al. (2007) evaluated *Opuntia-Ficus-Indica* (Nopal) mucilage as a corrosion inhibitor for steel in chloride-contaminated alkaline solutions, and the corrosion resistance improvement was apparently due to a denser oxide/hydroxide film formation on the reinforcing steel when Nopal mucilage reacted chemically with the metal, which, in turn, inhibited pit formation when chlorides were added to the electrolyte. Natural polymers are high molecular weight materials. Generally, there are 2 groups in natural polymers: polysaccharides and proteins [27]. Mucilage, a viscous heteropolysaccharide material, is generally obtained from plant stems. The monomer proportion in the molecules varies depending on the variety, age, environmental conditions and structure (fruit, cladode, rind), among other factors. It has applications in the food industry as an additive; in construction materials to improve stability and compressibility; in the cosmetic industry; in water purification processes as a flocculant; in the treatment of diabetes, gastritis and hyperglycemia; in house paints to improve the adhesiveness; and as an edible coating for fruits, among many other uses [28].

A group of plants that exhibit important antioxidant activities are Opuntias. These properties are attributed to their content of antioxidants, such as betalains, flavonoids, vitamins and phenolic compounds [29-30]. Centering in on the polyphenolic compounds that *Opuntia streptacantha* reportedly has, (4-hydroxy)-phenyl acetic acid is an organic compound that contains two functional groups: a phenyl and a carboxyl [31]. These compounds contain many oxygen atoms in functional groups, π-electrons and heterocyclic rings, which are reasons for the inhibition effect [32]. They adsorb ions on the coating/solution interface in the following ways: 1) donor-acceptor interactions between the π-electrons of aromatic rings and vacant d-orbitals of surface iron atoms and 2) interactions between unshared electron pairs of heteroatoms and vacant d-orbitals of iron surface atoms. These processes drastically reduce the transport of aggressive ions to the metal surface, thereby controlling the corrosion of carbon steel [32]. Organic compounds containing O, S, N, or their combinations, are reported as corrosion inhibitors for metals in acidic and alkaline solutions. The combination of these compounds in coatings protects a metallic surface and reduces chloride ion attack.

The efficiency of polymeric materials as corrosion-resistant coatings for metals increases when polymeric ligands are modified using corrosion inhibitors. Inhibitor compounds contained in a polymeric net could be used to create a group of coatings that respond to changes in the coating environment. The goal is to create inhibitors that are activated by the corrosion process itself, avoiding the exit of corrosive species from the coating. With this restriction, it is possible to reach the dual goal of corrosion protection by a barrier and the inhibition of metallic elements. From the available methodologies for evaluating the coating efficiency, weight loss measure (WLM), electrochemical impedance spectroscopy (EIS), linear polarization resistance (LPR) and potentiodynamic polarization curves (PDP) are prominent.

The goal of the present work is to produce a hybrid corrosion-resistant coating from cacti mucilage that forms a natural polymeric net for use as a coating on reinforced steel for concrete structures in high-chloride environments. This coating was characterized through instrumental analysis, and its electrochemical performance was evaluated.

2. EXPERIMENTAL

2.1 Sample preparation

Providing a clean surface allows proper coating adhesion. A grade 42 bar was the base material used for the working electrode (WE), which meets the Mexican standard NMX-C-407 and the American standard ASTM-A-615 / A 615M. Rebars with a 3/8" diameter were cut into 4 cm length sections and then cleaned to ensure an oxide and grease free surface. First, the rebar sections were immersed in 8% v/v hydrochloric acid solution for 10 minutes to remove surface rust. Subsequently, an ultrasonic cleaner treatment of the rebar sections in distilled water was conducted to remove any traces of acid on the metallic surface. Then, the rebar sections were dried using a heat gun. The rebar sections were placed in a desiccant with silica gel in preparation for the organic coating.

2.2 Mucilage extraction and coating formulations

In this study, cacti *Opuntia streptacantha* from the Epazoyucan region in Hidalgo, Mexico, were used. Cladodes with ages between 2 and 3 years old were considered, since they contain the highest concentrations of mucilage according to previous studies [16]. Mucilage extraction was performed according to a previously reported method (Ramírez y col., 2013), with a few modifications. After the mucilage extraction, the coating formulation was made with the following process: in an Erlenmeyer flask, mucilage, deionized water (18 MΩ cm^{-1}) and glycerol were added; the blend was heated at 90 °C for 5 minutes with constant stirring at 1200 rpm and then cooled to 25 °C, followed by the addition of polysorbate 80; finally, the mix was stirred for 5 minutes at 70 °C and 2000 rpm.

2.3 Electrochemical cell

The electrochemical cell arrangement was composed of the rebar segment as a WE. The WE had a nominal surface area of 5.4 cm^2 of steel in contact with the electrolyte, a coated or an uncoated sample depended on the test. The WE was immersed in a 3.5 wt.% NaCl solution. A graphite bar was used as the counter electrode, and a saturated calomel electrode was implemented as the reference electrode. Electrical connections of each bar specimen were made using copper wire. The experiments (all at 22 ± 2 °C) had two consecutive stages prior to their evaluation: 1) three-day drying periods for the rebar coating; and 2) a stabilization stage, in which the specimens were placed inside an electrochemical cell until the rebar stabilization potential was achieved (24 h).

2.4 Electrochemical measurements

Steel bar potential measurements were performed using a 500 MΩ impedance DC voltmeter (Fluke 289). They were measured versus a saturated calomel electrode (SCE) placed inside the cell. The measurements of PDP were performed after 24 hours of exposure to a 3.5% NaCl solution with the potential scanned between −2.5 V and +2.5 V at a rate of 1 mV s^{-1}. All electrochemical measurements

were performed at room temperature (22 ± 2 °C). EIS measurements were performed in a 3.5 wt.% NaCl using a saturated calomel electrode as the reference electrode and a graphite bar as the counter electrode. All EIS measurements were performed with a BioLogic SP-150 at a free corrosion potential. The AC frequency was swept between 200 kHz and 0.01 Hz with the rms width of the sinusoidal voltage signal applied to the system as 10 mV (9 points decade^{-1}).

2.5 Microscopic analysis

A steel bar microscope analysis was performed before and after the electrochemical tests. The rebar surfaces were photographed using an optical microscope. Segments of the steel bar surfaces were photographed. The segment micrographs were studied, and comparisons were made.

2.6 Coating formulation

Four different formulations were made (see Table 1) by varying the mucilage content with 0.2, 0.3, 0.4 and 0.5 g. The obtained hydrocolloid was placed in Eppendorf tubes to later be placed on the reinforced steel surface.

Table 1. Mucilage coating formulations for the uncoated steel.

Formulation	Formulation 1, **R1** (g)	Formulation 2, **R2**, (g)	Formulation 3, **R3**, (g)	Formulation 4, **R4**, (g)
Deionized water (18 MΩ cm-1)	20	20	20	20
Mucilage	0.2	0.3	0.4	0.5
Tween-80	0.4	0.4	0.4	0.4
Glycerol	0.4	0.4	0.4	0.4
Carboxymethylcellulose	0.1	0.1	0.1	0.1

Four different formulations were used to coat the rebar sections, with mucilage obtained from *Opuntia streptacantha* cacti as the base component. Rebar sections were coated by immersion and then dried at room temperature for three days to monitor the coating thickness.

3. RESULTS AND DISCUSSION

3.1 Coating thickness

Coating thickness was measured using an ultrasonic thickness-measuring tool (model Bruter NDT). The measurements were taken from 10 random spots on the coated surface, and the average value

was calculated; the obtained coating thickness was 18.75 µm. The coating process was performed by immersing the 0.9525 cm (3/8") diameter and 4 cm long rebar sections in the liquid formulation for 10 seconds before slowly removing the rebar. Afterwards, the working electrodes were dried for 72 hours at room temperature. Four test subjects from each formulation were evaluated in the electrochemical tests to guarantee reproducibility.

3.2 Corrosion studies

PDP for the four samples with coatings and a bare sample without a coating are given in Figure 5. The four samples with coatings and the bare sample exhibited active-to-passive behavior, where the greatest E_{corr} value was for R4, close to -500 mV, whereas the most active value was for R2, -667 mV, which was expected due to the lower mucilage content in the coating. The lowest corrosion current density value (27.59 mA cm^{-2}) was for R4 containing 0.5 g of mucilage, whereas the highest value (96.55 mA cm^{-2}) was for the bare sample. Additionally, the R1 coating showed a similar corrosion current density value (I_{corr}) to that of R4. Table 2 summarizes these values. The presence of coatings in the steel in a NaCl solution caused a shift in the E_{corr} toward an anodic value (more positive) compared to that of the blank, but no definite shift in the E_{corr} values was observed. The magnitude of change in the E_{corr} values suggested that mucilage in a coating acts as an inhibitor with predominantly anodic effects, i.e., an anodic dissolution of carbon steel is more favored than a cathodic evolution of hydrogen gas [33]. The value of I_{corr} decreased with increasing mucilage concentration in the coating, suggesting that in the presence of mucilage, the rate of electrochemical reaction was slowed due to the protective film on the carbon steel surface, which created a barrier between the metal and corrosive NaCl solution. Considering the variation in the Tafel slope values (Table 2), apart from R4, the values of βc did not change much. However, the values of βa varied in a regular manner. The change in βa values was better than the change in the βc values, indicating that the coating suppressed the anodic reaction to greater extents than the cathodic one. The mucilage in the coating might have formed a protective film that acted as a physical barrier to control the diffusion of ions to the steel surface and consequently slowed the corrosion process. It seems that with mucilage concentration, only the anodic dissolution reaction is slowed, whereas with an increase in mucilage concentration, both the anodic and cathodic reaction rates diminish.

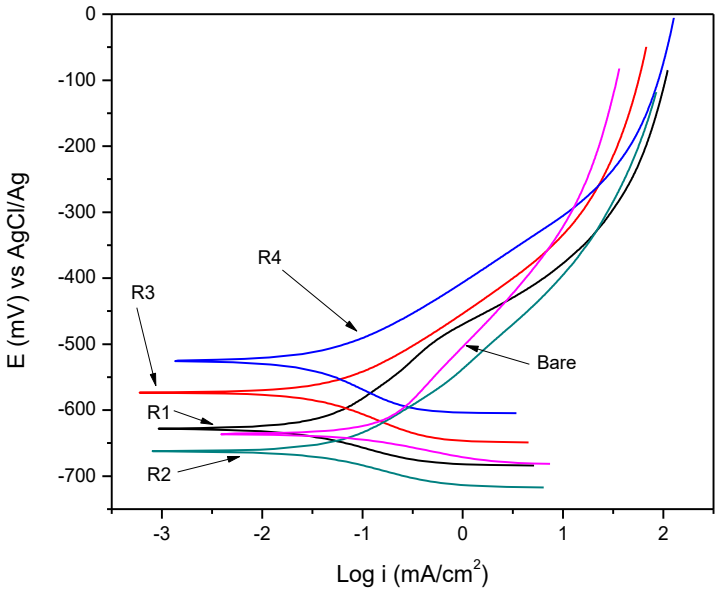

Figure 5. Effect of mucilage content on the PDP for coated steel and bare steel without a coating in 3.5 wt.% sodium chloride at 25 °C.

Table 2. Electrochemical parameters obtained from PDP.

Sample	E_{corr} vs Ag/AgCl (mV)	I_{corr} (μA/cm^2)	βa (mV/decade)	βc (mV/decade)	*η%*
R1	-633.816	27.6	92.7	41	71.41
R2	-667.756	39.472	80.8	39.3	59.11
R3	-578.7	34.495	77.3	59.6	64.27
R4	-528.894	27.593	68	71.1	71.42
Bare	-643.328	96.555	111.7	24.8	--

3.3 EIS analysis

Electrochemical impedance spectroscopy (EIS) at a corrosion potential was used to characterize the coating on the metal substrate (rebar). Figure 6 shows the EIS spectrum behavior according to immersion time. EIS data fit the classic equivalent electrical circuit model with one RC time constant distributed hierarchically to describe the coating immersed in the electrolyte, using equation 1 as a model for general impedance [31,32]:

$$Z(\omega) = R_1 + \frac{R_2}{R_2 C_2 (j2\pi\omega)^{\alpha_2} + 1}; \quad \text{(Eq. 1)}$$

where R_1 is the electrolyte resistance and R_2C_2 is the medium-low frequency time constant, which is related to the dielectric properties of the coating (barrier properties). For uncoated steel, R_2C_2 is the low-frequency time constant related to the redox process that takes place in the coating-metal interface and i parameters consider the time constants of the R_iC_i Cole-Cole dispersion.

3.3.1 Nyquist

EIS data in a Nyquist format reveal interesting characteristics on the organic coating behavior and the uncoated rebar. Figure 6 shows that for all cases, the data describe an unfinished capacitive semicircle, starting at a low frequency and having their centers in the real axis at medium frequencies. Semicircle existence is related to a protective element, which are the organic coatings in the coated steel and the passive layer in the uncoated steel. All cases present a similar behavior, as shown in Figure 5, which indicates that the corrosion process is controlled by charge transfer. For that process, the linear polarization resistance value, R_p, equals the semicircle diameter, or the coating resistance (R_{pore}) for coated steel, and the charge transfer resistance (R_{ct}) for bare steel. The higher semicircle diameters are for the organic coatings, ordered from the higher value: R1, R4, R2, R3 and bare. There is a deviation from a perfect semicircle, a depressed semicircle in the center under the real axis that is due to the state of the electrode surface and the dispersion effect, which is a typical impedance feature of carbon steel electrodes in a corrosion process [34]. The impedance response of the working electrode changed significantly after the addition of varying concentrations of mucilage in the coatings used in the immersion solution. The shapes of the impedance plots for the electrodes with or without coatings were not different, except for their diameter, which indicated that the addition of the mucilage coating caused a significant change in the mechanism of corrosion [35].

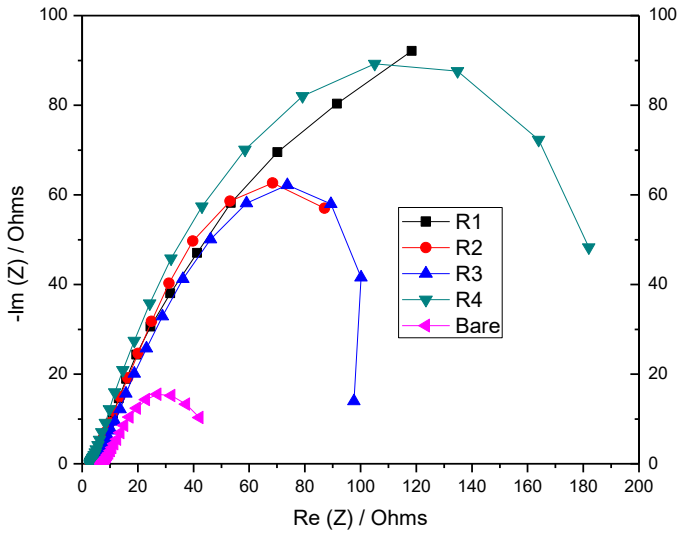

Figure 6. EIS Nyquist diagrams for the coated and uncoated steel after 24 h in a 3.5 wt.% NaCl solution.

3.3.2 Bode

Figure 7 shows the coatings and bare steel behavior in a 3.5 wt.% NaCl in Bode diagrams with the impedance module $|Z|$ against frequency. At short time lapses (1 h) there is a single time constant in the system. The single time constant appears as a straight line with a slope close to -1 at the medium-low frequencies region, followed by a straight line parallel to the x axis at high frequencies. Coating resistance at the pores (R_{pore}) is related to a conductive path within the coating heterogeneities, and

together with a constant phase element (CPE_{coat}), they are related to a passive layer and a coating. At short exposure times, the impedance value $|Z|$ at the lowest frequencies corresponds only to the R_{pore} value, although the straight line at high frequencies is related to the solution resistance R_{sol}. Consequently, the time constant defined by R_{pore} and CPE_{coat} causes this kind of figure in the impedance module against the frequency diagram. It is shown in Figure 7 that the highest CPE_{coat} value was obtained by formulation R4, followed by R3, R1, R2 and finally the uncoated steel. It is also observable in the trend of R_{pore} values, with the R4 formulation obtaining the highest value, followed by R1, R3, R2 and the uncoated steel, which had the lowest impedance module value. The existence of a time constant in a steel immersed in a high-chloride solution indicates a barrier effect, which decelerates the metallic corrosion process. In the Bode phase plot (Figure 7), where the phase angle vs. frequency is plotted, the phase angle at high frequencies provides a good idea of the inhibitory effect of the compound. Higher protection for steel with a mucilage coating was obtained in the presence of a solution of 3.5 wt.% NaCl, with an increase in values of absolute impedance at low frequencies [36].

Figure 8 shows the angle phase evolution against the frequency logarithm for the coatings and bare rebar. At short exposure times, there was a time constant with a maximum point in the described curves. According to scientific studies, this behavior is caused by a semi-infinite diffusion phenomenon contribution at the pores, tangential electrolyte penetration in the interphase metal/coating, and a distribution in relaxation times due to heterogeneous penetration by the electrolyte. In the theta vs. frequency diagram (Figure 8), increasing negative values of the phase angle at high frequencies are observed with an increase in the coating mucilage concentration in the test solution. A more negative phase angle corresponded to more capacitive electrochemical behavior. The capacitive response was enhanced with the presence of mucilage, indicating more inhibitory behavior at higher concentrations [37].

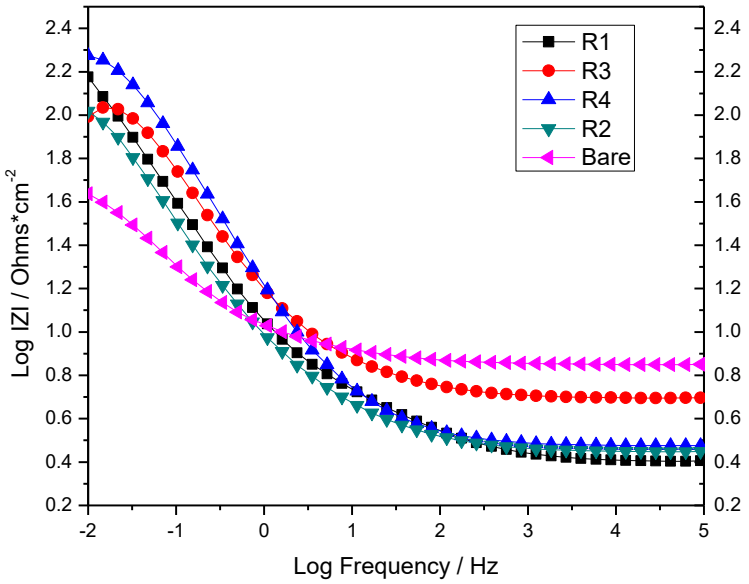

Figure 7. EIS Bode diagrams for the coated and uncoated steel after 24 h in a 3.5 wt.% NaCl solution.

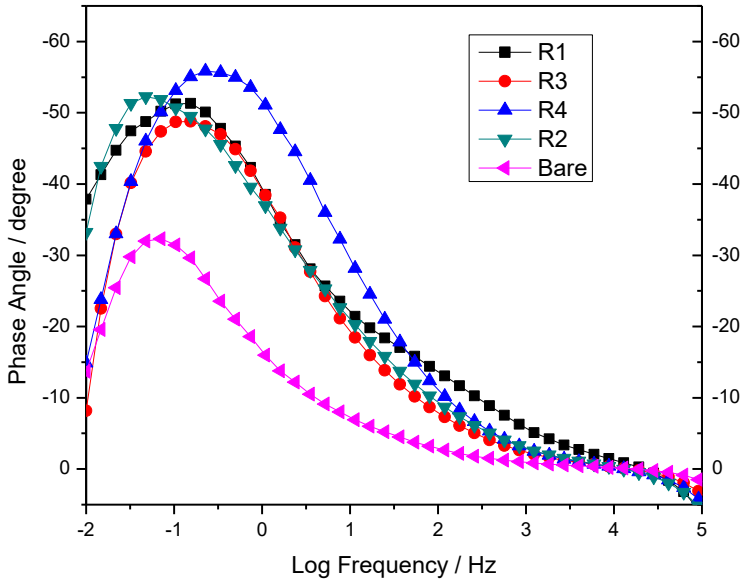

Figure 8. EIS Bode (Phase Angle) diagrams for the coated and uncoated steel after 24 h in a 3.5 wt.% NaCl solution.

3.3.3 Equivalent Circuit

EIS results for the organic coatings can be presented with physical elements in an equivalent circuit. The circuit in Figure 9(a) is formed by a resistance, R_s, which represents the solution resistance and a constant phase capacitor, CPE_{coat}, connected in parallel with the coating resistance, R_{coat}. Additionally, an equivalent circuit is proposed for the uncoated steel shown in Figure 9(b); it is a charge-transfer constant phase element parallel circuit (CPE_{ct}), and its charge transfer resistance (R_{ct}) is associated with a typical uncoated steel in aggressive media redox reactions. The electrochemical impedance parameters were determined by a semicircle fitting method [38]. Electrical parameters were fitted by EC-Lab software (EC-Lab®) using a randomize-simplex numeric generator and are presented in Table 3.

The described impedance diagrams behavior obtained by equivalent circuit simulation is summarized in Table 3, which shows that the R4 organic coating has the highest resistance (R_{pore}) and that bare steel has the lowest resistance. However, CPE_{coat} (n) values demonstrated that the passive layer behaves as a nonideal coating, which means that its resistance is lower due to its nature as a layer of corrosion products. This parameter is related to the Nyquist diagram semicircle geometry or capacitive behavior, which is in the range from 0 to 1. Considering n=0, the signal potential of the current passes through the system and behaves as a resistor; thus, CPE is a resistor. However, for n=1, the signal potential of the current passes through a system and behaves as a capacitor; thus, CPE is a capacitor. Finally, system ideality deviations are assessed, that is, when $n>0$ but $n<0.5$ or $n>0.5$ but $n<1$. These values are related to surface characteristics, such as roughness, porosity or heterogeneity in coatings. All the formulations presented $n>0.5$, which is related to the coating porosity that allows electrolytes to flow

through the coating and is related to the corrosion products on the metallic surface of the bare steel [39,40].

Figure 9. Equivalent circuit model, (a) the coated steel and (b) uncoated steel.

Table 3. Electrochemical impedance data for the coated and uncoated steel in a 3.5% NaCl solution.

System	R_s (Ω)	R_{coat} (Ω)	CPE_{coat} [F.s^(n - 1)]	n
R1	2.691	358.6	0.03175	0.6523
R2	3.029	164.4	0.03819	0.7412
R3	5.101	162.4	0.02226	0.6618
R4	3.068	275.8	0.01704	0.7112
System	R_s (Ω)	R_{ct} (Ω)	CPE_{dl} [F.s^(n - 1)]	n
Bare	7.196	63.2	0.07381	0.5823

3.4 Inhibition efficiencies

The electrochemical techniques PDP and EIS were used to evaluate coating behavior in a high chloride environment. Moreover, a parameter determination was also conducted to characterize each coating. Different coating formulations were prepared and then evaluated for their inhibitory performance by a potentiodynamic polarization technique. Corrosion current density (I_{corr}) and corrosion potential (E_{corr}) were measured from PDP by a Tafel extrapolation method.

The percentage of inhibition (η) was calculated according to equation 2:

$$\eta\% = \frac{[(Icorr - Icorr\ (coating)]}{Icorr} * 100\ ; \qquad \text{(Eq. 2)}$$

where $I_{corr(coating)}$ and I_{corr} are the corrosion current densities of the coated and uncoated rebar electrodes, respectively. The results are shown in Figure 5, and their related parameters are reported in Table 2. Figure 5 displays the PDP for bare steel and for coated steel with different formulations and ambient temperatures.

Inhibition efficiencies [E (%)] were determined based on the following equation [41]:

$$E(\%) = \frac{R_{coat} - R_{ct}}{R_{coat}} * 100\ ; \qquad \text{(Eq. 3)}$$

where R_{ct} is the charge transfer resistance without coating and R_{coat} is the charge transfer resistance with coating. The R_{ct} and R_{coat} values were determined as the diameter of the semicircles from the Nyquist plots. The results are shown in Table 4, and their related parameters are reported in Table 3. The highest efficiency value was obtained by the R1 coating, and the lowest by the R3 coating, with higher mucilage concentrations presenting higher efficiency, which indicates the feasibility of mucilage

coatings to act as inhibitors. Thus, at mucilage concentrations of 0.3 and 0.4 g, the inhibitor of metal electron transfer dominates (except at 0.2 g), whereas at higher concentrations, back donation starts. Inhibition efficiency increases with an increasing mucilage concentration. The inhibition efficiencies obtained from the IES and PDP measurements were the highest with inhibition efficiency values of 82.37 and 71.42% at mucilage concentrations of 0.2 and 0.5 g, respectively. The inhibition efficiencies obtained from the polarization measurements of the cactus plant extracts displayed the same trend as those calculated from the gravimetric measurements [38,42-45]. On the basis of these data, mucilage can be considered a good inhibitor in a coating for the corrosion of low carbon steel in a 3.5% NaCl solution at comparatively lower concentrations and room temperature.

Table 4. *Opuntia streptacantha* inhibitor coating efficiency values.

System	E(per cent)
R1	82.375906
R2	61.557178
R3	61.083744
R4	77.084844

3.5 Microscopy

Coated steel specimen morphology (R4 and R1) and uncoated steel in a 3.5 wt.% NaCl solution were observed with a metallographic microscope and a 100X lens (Figure 10) before the PDP was performed and after the polarization curve technique, sonication in deionized water cleaning and heat gun drying. According to micrographs, corrosion products are visible in greater surface zones for the uncoated steel, while there is no corrosion damage on the coated metallic surfaces. However, organic coatings present surface degradation, and chloride ions can diffuse through the coating surface using the coating porosity as a passage, causing coating loss by delamination.

(a) Before

(b) After

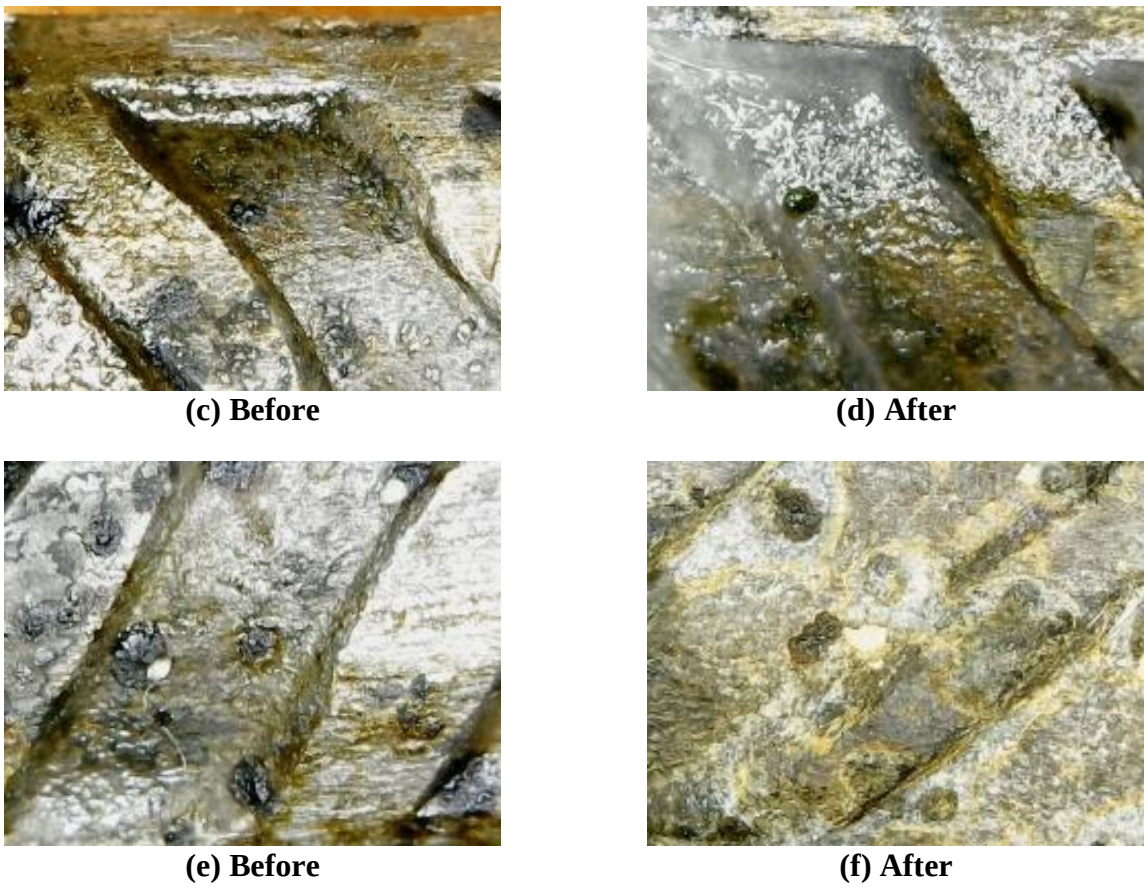

(c) Before **(d) After**

(e) Before **(f) After**

Figure 10. Micrographs; (a) before and (b) after the uncoated steel surface electrochemical tests; (c) before and (d) after the R1 coating electrochemical tests; and (e) before and (f) after the R4 coating electrochemical tests, in a 3.5 wt.% NaCl solution.

Chloride ions attack uncoated steel surfaces preferring defect surface zones, promoting localized damage and augmenting the amount of corrosion products on the metallic surface. Hernandez et al. (2017) used reinforcement rebar steel to evaluate organic corrosion inhibitors, and all control rebars presented larger pits compared to those in the organic additive solutions (CM = cactus mucilage extract, CN = calcium nitrite) [46]. When the electrolyte arrives at the coating/metal interphase, electrochemical reactions start to take place. All the formulations act as a barrier reducing the chloride ion diffusion rate, and hence, the localized corrosion damage on the metal surface decreases. Formulations R4 and R1 present more acceptable barrier properties, less coating surface damage and smaller corrosion product zones.

3.5 Discussion

No uncoated zones were detected on the assessed organic coated steel electrodes, which indicates that there was adequate surface adhesion due to a proper surface preparation. The coating barrier ability prevented the physicochemical interactions between the solution and the coating and was conditioned to solution diffusion. Organic coatings did not present damage by blistering or cracking. However, coating

adhesion allows for the prediction of a coating corrosion mechanism. Delamination occurs when water, salts or contaminant agents agglomerate in the coating due to coating permeability or to coating defects. Delamination can lead to organic polymer degradation, which promotes electrolyte permeability to the metallic surface and can cause localized corrosion attack at long exposure times. Inhibitor effectiveness is susceptible to the adhesion of chloride ions to the phenolic and flavonoid molecules existing in the mucilage. In the easiest case, it can be considered that phenol molecules can transform into a 2,4,5-trichlorophenol by the adhesion of 3 chloride ions. The study showed that the presence of mucilage molecules in rebar carbon steel surface coatings in the test solution is mixed adsorption, either by electrostatic interaction of the polymer with a positively charged carbon steel surface [47-49] or through the lone pairs of electrons on oxygen atoms and chlorides. Initially, the protonated mucilage molecules interact electrostatically with the positively charged carbon steel and later with chlorides. This reflects the influence in the adsorption process of organic inhibitors on chloride ions. Cl ions do not need to be very hydrated and have a stronger tendency to be adsorbed on the metal surface compared to other ions. Additionally, chloride ions have the ability to create an excessive negative charge toward the solution phase, which favors the adsorption of organic species of Cl ions on the metal surface and the generation of pitting [50-52]. The coating advantage reflects the influence of the hybrid coating with chloride ions in the adsorption process that prevents the chloride ions from reaching the metal surface.

The presented results show that the cacti mucilage-based coating formulations are effective corrosion inhibitors for steel in high chloride concentration environments. This is explained by the capability of the mucilage to distribute homogeneously within the coating. The coating acts as a barrier between the solution and the metallic surface, which inhibits the redox reactions and suppresses the charge transfer on the steel surface, decelerating the corrosion process.

4. CONCLUSIONS

Cacti mucilage was dispersed successfully on an organic coating matrix at concentrations of 0.2, 0.3, 0.4 and 0.5 g. Electrochemical evaluation of steel in a 3.5 wt.% NaCl solution presented promising corrosion inhibition properties, where the formulation with the highest mucilage content (R4 coating) presented the best inhibition behavior.

Electrochemical measurements also showed that mucilage could be considered an effective inhibitor. The inhibition efficiencies obtained from the PDP and the EIS concur and confirm the steel protection shown in the micrographs. Electrochemical measurements showed that the mucilage coating behaved as a barrier layer on the carbon steel (reinforcing steel) surface, protecting it from an aggressive NaCl medium.

The coatings present an acceptable resistance to crack initiation and propagation. This resistance limits the generation of localized coating defects, appearance deterioration and mechanical resistance. Coating porosity allows solution entry; however, the organic compounds present in the mucilage of the coating interact with chloride ions, reducing the chloride ions available to attack the metallic substrate, thus limiting localized corrosion. This does not limit the water entry through the coating pores.

The results show that coatings based on mucilage obtained from *Opuntia streptacantha* are useful for improving the corrosion resistance of steel in aggressive environments with high chloride ion concentrations. This is promising for future studies where the formulations could be improved by adding higher concentrations of mucilage, higher exposure times and assessing the obtained superficial compounds.

ACKNOWLEDGEMENTS
The authors wish to thank the Ministry of Education (SEP-PRODEP) for the support provided to both the Academic Body "Ingeniería Civil Sustentable y Tecnología de Materiales", UAEH-CA-87.

References

1. J.G. Cabrera, *Cem. Concr. Res.,* 18 (1996) 47.
2. A. Tamer, E. Maaddawy, A. Khaled and Soudki, *J. Mater. Civil Eng.,* 15 (2003) 899.
3. L. Dawang, R. Wei, L. Li, G. Xiaotao and M. Xuming, *Constr. Build. Mater.,* 199 (2019) 359.
4. M.C. Alonso, F.J. Luna and M. Criado, *Constr. Build. Mater.,* 199 (2019) 385.
5. U. Angst, B. Elsener, C.K. Larsen and O. Vennesland, *Cem. Concr. Res.,* 39 (2009) 1122.
6. A.Y. El-Etre, M. Abdallah and Z.E. El-Tantawy, *Corros. Sci.,* 47 (2005) 385.
7. F. Galliano and D. Landolt, *Prog. Org. Coat.,* 44 (2002) 217.
8. A. Hartwig, M. Sebald, D. P¨utz and L. Aberle, *Macromol. Symp.,* 221 (2005) 127.
9. B. Wetzel, F. Haupert and M.Q. Zhang, *Compos. Sci. Technol.,* 63 (2003) 2055.
10. N. Saurín, J. Sanes and M.D. Bermúdez, *Tribol. Lett.,* 58 (2015) 4.
11. L. Bertolini, B. Elsener, P. Pedeferri, E. Redaelli and R.B. Polder, *Corrosion of Steel in Concrete*, John Wiley & Sons Inc, (2013) Weinheim, Germany.
12. W. Morris, M. Vazquez and S.R.D. Sanchez, *J. Mater. Sci.,* 35 (2000) 1885.
13. N. Gowripalan and H.M. Mohamed, *Cem. Concr. Res.,* 28 (1998) 1119.
14. P. Pokorný, P. Tej and M. Kouil, *Constr. Build. Mater.,* 132 (2017) 271.
15. G. Markeset, S. Rostam and O. Klinghoffer, *Guide for the use of stainless steel re-inforcement in concrete structures*, Tech. Rep. Norwegian Building Research Institute, (2006) Oslo, Norway.
16. T. Wanotayan, Y. Boonyongmaneerat, J. Panpranot, E. Tada and A. Nishikata, ISIJ International, 58 (2018) 1316.
17. P.C. Dodds, G. Williams and J. Radcliffe, *Prog. Org. Coat.,* 102 (2017) 107.
18. N.O. Eddy and S.A. Odoemelam, *J. Mater. Sci.,* 46 (2011) 5208.
19. S.A. Umoren, I.B. Obot, E.E. Ebenso and N.O. Obi-Egbedi, *Electrochim. Acta,* 26 (2008) 199.
20. E.E. Oguzie, *Mater. Lett.,* 59 (2005) 76.
21. D. Zhao, J. Sun, L. Zhang, Y. Tan and J. Li, *J. Rare. Earth.,* 28 (2010) 371.
22. M. Ozcan, R. Solmaz, G. Kardas and I. Dehri, *Colloids Surf.,* 325 (2008) 57.
23. C. Sáenz, E. Sepúlveda and B. Matsuhiro, *J. Arid Environ.,* 57 (2004) 275.
24. M. Aguirre, P. García, R. González, A.L. Jofre, A.V. Legorreta and J.F. Buenrostro, *Desarrollo y evaluación de una película comestible obtenida del mucílago del nopal (Opuntia ficus indica) utilizada para reducir la tasa de respiración de nopal verdura*, VIII Congreso Iberoamericano de Ingeniería de Alimentos, Lima, Perú, 2011, 1.
25. A.Y. El-Etre, *Corros. Sci.,* 45 (2003) 2485.
26. K. Tebbji, H. Oudda, B. Hammouti, M. Benkaddour, M. El-Kodadi and A. Ramdani, *Colloids Surf.,* 259 (2005) 143.
27. J.C. Ruiz, M.R. Segura, *New Polymers for Encapsulation of Nutraceutical Compounds*, John Wiley

& Sons, Inc., (2017) Hoboken, USA.
28. V. Del-Valle, P. Hernández, A. Guarda and M.J. Galotto, *Food. Chem.,* 91 (2005) 751.
29. A. Piga, *J. Pro. Asoc. Cac.,* 6 (2004) 9.
30. L. Santos, J.A. Gutiérrez and S.O. Serna, *J. Agric. Food Chem.,* 59 (2011) 7054.
31. A. Andrade and H. Wiedenfeld, *J. Ethnopharmacol.,* 133 (2011) 940.
32. M. Zhao, N. Yang, B. Yang, Y. Jiang and G. Zhang, *Food. Chem.,* 105 (2007) 1480.
33. M. Hany, E.L. Abd, *Corros. Sci.,* 92 (2015) 104.
34. I.S. Cole, D. Marney, *Corros. Sci.,* 56 (2012) 5.
35. E. Bayol, T. Gurten, A.A. Gurten and M. Erbil, *Mater. Chem. Phys.,* 112 (2008) 624.
36. P. Bommersbach, C. Alemany-Dumont, J.P. Millet and B. Normand, *Electrochim. Acta,* 51 (2006) 4011.
37. K.F. Khaled and N. Hackerman, *Electrochim. Acta,* 48 (2003) 2715.
38. B. Zhang, C. He, X. Chen, Z. Tian and F. Li, *Corros. Sci.,* 90 (2015) 585.
39. A. Lasia, *Modern Aspects of Electrochemistry*, Springer, (2002) Boston, USA.
40. J. Baptiste, E.M. Orazem, N. Pébere and B. Tribollet, *Electrochim. Acta,* 51 (2006) 1473.
41. G. Gonzalez, J. Martinez, F.A. Dominguez, G. Suarez, *Anti-Corros. Method. M.,* 61 (2014) 224.
42. Z. Ghazi, H. ELmssellem, M. Ramdani, A. Chetouani, R. Rmil, A. Aouniti, C. Jama and B. Hammouti, *J. Chem. Pharm. Res.,* 6 (2014) 1417.
43. E. Honarmand, H. Mostaanzadeh, M.H. Motaghedifard, M. Hadi and M. Khayadkashani, *Prot. Met. Phys. Chem.,* 53 (2017) 560.
44. Z. Ghazi, H. ELmsellem, M. Ramdani, A. Chetouani, R. Rmil, A. Aouniti, C. Jama and B. Hammouti, *J. Chem. Pharm. Res.,* 6 (2014) 1417.
45. I.O. Arukalam, I.C. Madufor, O. Ogbobe and E.E. Oguzie, *Pigm. Resin. Technol.,* 43 (2014) 151.
46. E.F. Hernández, P.F.J. Cano, F.M. León, A.A. Torres, *Anti-Corros. Method. M.,* 64 (2017) 529.
47. A.O. Yuce and A.G. Kardas¸ *Corros. Sci.,* 58 (2012) 86.
48. D. Addari, B. Elsener and A. Rossi, *Electrochim. Acta,* 361 (2019) 280.
49. A.A. Torres, *J. Appl. Electrochem.,* 37 (2007) 835.
50. E.I. Ating, S.A. Umoren, I.I. Udousoro, E.E. Ebenso and A.P. Udoh, *Green Chem. Lett. Rev.,* 3 (2010) 61.
51. N.A. Odewunmi, S.A. Umoren and Z.M. Gasem, *J. Ind. Eng. Chem.,* 21 (2015) 239.
52. E.A. Noor, *Int. J. Electrochem. Sci.,* 2 (2007) 996.